The Male Determinant of Self-Incompatibility in *Brassica*

Christel R. Schopfer, Mikhail E. Nasrallah, June B. Nasrallah*

In the *S* locus–controlled self-incompatibility system of *Brassica*, recognition of self-related pollen at the surface of stigma epidermal cells leads to inhibition of pollen tube development. The female (stigmatic) determinant of this recognition reaction is a polymorphic transmembrane receptor protein kinase encoded at the *S* locus. Another highly polymorphic, anther-expressed gene, *SCR*, also encoded at the *S* locus, fulfills the requirements for the hypothesized pollen determinant. Loss-of-function and gain-of-function studies prove that the SCR gene product is necessary and sufficient for determining pollen self-incompatibility specificity, possibly by acting as a ligand for the stigmatic receptor.

In self-incompatible plants of the genus *Brassica*, self-related pollen grains are recognized and prevented from germinating by interaction with the epidermal cells of the stigma, the receptive surface of the female reproductive organ. This self-incompatibility (SI) phenomenon is genetically controlled by a complex and polymorphic locus (*1*, *2*). Among the genes at this *S* locus is a pair of sequence-related genes, the cell wall–localized *S*-locus glycoprotein (*SLG*) gene and the plasma membrane–spanning receptor protein kinase (*SRK*) gene, both of which are expressed specifically in the stigma epidermal cells. Different variants of the *S* locus, designated *S* haplotypes, are characterized by highly polymorphic alleles for *SLG* and *SRK* (*1*, *3*, *4*). Although one function of SLG is to stabilize SRK, SRK itself is viewed as a ligand-activated receptor kinase and the primary female determinant of SI (*1*, *5*). Selective binding of a pollen-borne ligand is thought to initiate a signal transduction cascade resulting in the SI pollen rejection reaction. This view requires that the *S* locus contain at least one more SI gene, an as-yet unidentified gene that would encode the male determinant and provide directly or indirectly the ligand for the SRK receptor (*6*–*8*).

Recombination analysis of the *B. campestris* (synonym *B. rapa*) S_8 haplotype has shown that the male and female SI determinants are contained in a 65-kb chromosomal segment encompassing SLG_8 and SRK_8 (*2*, *7*). During sequence analysis of the 13-kb region between SLG_8 and SRK_8, we discovered that the 400–base pair (bp) Hind III–Xba I restriction fragment indicated in Fig. 1A contained a small segment with an unusually high frequency of cysteine residues in one of the deducible reading frames. RNA gel blot analysis with the 400-bp Hind III–Xba I fragment as probe revealed that this segment is part of a transcribed gene that is expressed specifically in anthers (see below). Indeed, screening of an S_8 anther cDNA library allowed the isolation of a 450-bp full-length cDNA clone. Sequence comparison of this clone and the SLG_8-SRK_8 intergenic segment determined that the gene consists of two exons (110 and 300 bp) separated by an unusually large intron of 4.1 kb (Fig. 1A). In DNA gel blot analysis, the 400-bp Hind III–Xba I probe detected restriction fragments with sizes predicted by the restriction map (Fig. 1B). Thus, we had identified a single-copy, *S* locus–encoded, anther-expressed gene, which we named *S* locus cysteine-rich protein (*SCR*) gene.

S Locus–Associated Polymorphism of *SCR*

We isolated *SCR* cDNA clones from the *B. oleracea* strains S_6 and S_{13} (*9*). These two cDNAs, designated SCR_6 and SCR_{13}, represent true *SCR* alleles because they detected the same size bands as the SCR_8 probe on *Brassica* DNA gel blots. Furthermore, SCR_6 and SCR_{13} cosegregated in F_2 populations, respectively, with the SLG_6/SRK_6 and SLG_{13}/SRK_{13} gene pairs as well as with S_6 and S_{13} SI specificities, demonstrating their genetic linkage to the *S* locus (*10*). The *S* haplotype association of *SCR* was also demonstrated by DNA gel blot analysis of other *S* homozygotes. Under low-stringency conditions, which were used in order to maximize the detection of possibly highly divergent alleles, most of the seven *S* homozygotes we analyzed exhibited a single band hybridizing with the *SCR* probe (Fig. 2A). However, the length of the restriction fragments varied between strains, consistent with the notion that the *SCR* gene exists as a single-copy gene localized at the polymorphic *S* locus. These results confirm that the *SCR* gene is a consistent feature of the *S* haplotype (*11*).

Examination of the DNA gel blots also revealed that the intensity of the hybridization signal, a qualitative indication of nucleic acid sequence similarity, showed *S* haplotype–associated variation. Under low-stringency conditions, an SCR_{13}-derived probe hybridized with DNA from the S_6, S_{13}, S_{14}, S_{22}, S_{29}, and S_8 homozygotes, albeit with varying degrees of intensity, but not with DNA from the S_2 homozygote (Fig. 2A). Only simultaneous hybridization with SCR_6 and SCR_8 allowed the detection of a weak hybridization signal in S_2 DNA (Fig. 2B). This pattern of *S* haplotype–associated variation mirrors that observed for the *SLG/SRK* gene pair: Alleles of this gene pair isolated from the S_6, S_{13}, S_{14}, S_{22}, S_{29}, and S_8 haplotypes share >85% DNA sequence similarity with each other but only <70% similarity with alleles isolated from the S_2 haplotype (*3*, *4*). The parallelism between *SCR* and *SLG/SRK* was also apparent in the hybridization patterns obtained with the SCR_{13} probe under high-stringency conditions, which resulted in the loss of hybridizing bands in all *S* homozygotes except for the *B. oleracea* S_{13} and *B. campestris* S_8 homozygotes (Fig. 2C). This relatively high interspecific sequence similar-

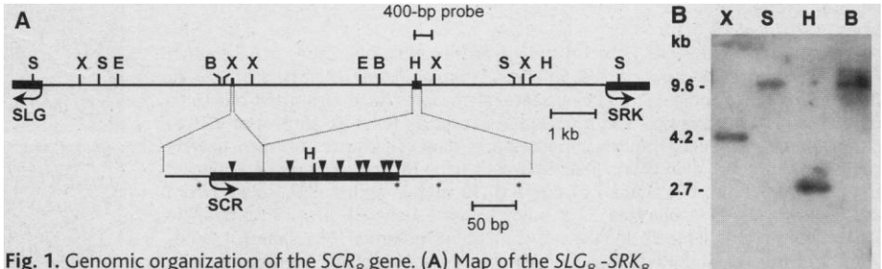

Fig. 1. Genomic organization of the SCR_8 gene. (**A**) Map of the SLG_8-SRK_8 intergenic region and of the SCR_8 cDNA. Restriction sites: B, Bam HI; E, Eco RI; H, Hind III; S, Sac I; and X, Xba I. The translation start sites of SLG_8, SRK_8, and SCR_8 are marked by arrows. Exons are indicated by filled boxes. The bar labeled "400-bp probe" indicates the Hind III–Xba I fragment used for hybridization experiments. The positions of cysteine codons in the SCR_8 cDNA are marked by arrowheads, and the positions of stop codons flanking the *SCR* open reading frame are marked by asterisks. (**B**) DNA gel blot analysis of SCR_8. Genomic DNA from S_8S_8 homozygotes, digested with Xba I (X), Sac I (S), Hind III (H), or Bam HI (B), was hybridized with the 400-bp probe (A).

Department of Plant Biology, Cornell University, Ithaca, NY 14853, USA.

*To whom correspondence should be addressed. E-mail: jbn2@cornell.edu

ity between SCR_{13} and SCR_8, verified by sequence analysis (see below), coincides with the observation that the *B. oleracea* SLG_{13}/SRK_{13} gene pair exhibits higher amino acid sequence similarity to *B. campestris* SLG_8/SRK_8 than to other *B. oleracea* *SLG/SRK*s such as SLG_6/SRK_6 (*4*). In conclusion, *SCR* appears to have coevolved with the *SLG/SRK* gene pair.

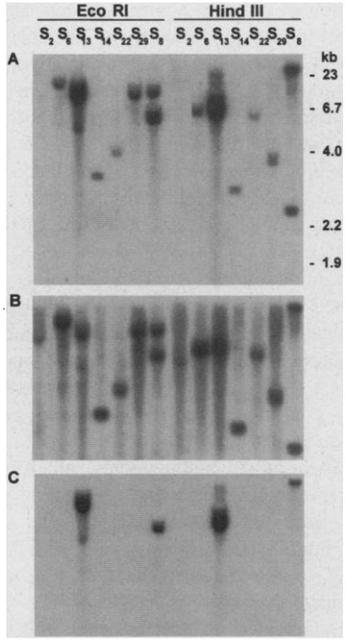

Fig. 2. DNA gel blot analysis of *SCR* in plants homozygous for the S_2, S_6, S_{13}, S_{14}, S_{22}, and S_{29} haplotypes of *B. oleracea* and the S_8 haplotype of *B. campestris*. Gel blots of DNA digested with Hind III or Eco RI were sequentially hybridized with the SCR_{13} probe at 65°C (**A** and **C**) and a combined SCR_6/SCR_8 probe at 55°C (**B**) and washed under low (A and B) or high stringency (C). Final wash solutions were (A) 2× SET, 0.5% SDS at 65°C, (B) 0.2× SSC, 0.2% SDS at 55°C, and (C) 0.2× SET, 0.1% SDS at 65°C.

Function as the Male Determinant of SI

To test whether *SCR* is indeed the male determinant of SI, we initiated a detailed analysis of both its expression and function. First, we analyzed the expression of *SCR* in wild-type self-incompatible plants by RNA gel blot analysis (*12*). *SCR* shows an anther-specific, developmentally regulated expression profile (Fig. 3A, lanes 1 to 6). *SCR* transcripts can be detected in anthers only after the generation of haploid microspores, with transcripts accumulating in the microspores (Fig. 3A, lane 7). Therefore, the *SCR* gene is active postmeiotically and gametophytically. However, our data do not exclude expression of *SCR* in sporophytically derived cells of the anther such as the tapetum, a secretory cell layer that lines the anther locule in which microspores develop and that is a source for several pollen coat components.

We also analyzed the accumulation of *SCR* transcripts in anthers isolated from a self-compatible mutant *B. oleracea* strain, designated *m1600*, which was generated by γ-irradiation of an $S_{13}S_{13}$ homozygote (*13*). Reciprocal pollinations between *m1600* and self-incompatible $S_{13}S_{13}$ plants had shown that the lesion in *m1600* resulted in the loss of S_{13} specificity in pollen but not in stigma. Gel blot analysis of anther RNA demonstrated that, in contrast to plants carrying the wild-type S_{13} haplotype, *m1600* anthers lacked detectable SCR_{13} transcripts (Fig. 3A, lanes 8 to 10). The correlation between loss of pollen S_{13} specificity and absence of detectable SCR_{13} transcripts in the *m1600* mutant strain provides strong evidence that *SCR* is necessary for pollen SI specificity.

To obtain definitive proof that *SCR* functions as the pollen determinant of SI, we transformed a *B. oleracea* S_2S_2 homozygous strain with a chimeric gene consisting of the SCR_8 promoter fused to the SCR_6 cDNA (*14*). Among 14 independent hygromycin-resistant plants, 12 plants expressed the SCR_6 transgene and were designated S_2S_2/SCR_6^+, whereas two plants failed to produce detectable levels of SCR_6 transcript and were designated S_2S_2/SCR_6^- (Fig. 3A, lanes 11 to 14). Pollination assays showed that the stigmas of the S_2S_2/SCR_6^+ and S_2S_2/SCR_6^- plants were compatible with pollen from S_6S_6 plants, a response identical to that of the S_2S_2 transformation host strain. Pollen from the two S_2S_2/SCR_6^- plants germinated and produced pollen tubes on S_6S_6 stigmas (*15*) (Table 1 and Fig. 3, C and F). In contrast, pollen from each of the 12 S_2S_2/SCR_6^+ plants was inhibited by S_6S_6 stigmas (Fig. 3, B and E), even though pollen was viable as demonstrated by its ability to elaborate pollen tubes on stigmas homozygous for an unrelated *S* haplotype such as S_{22} (Table 1). Thus, pollen of S_2S_2/SCR_6^+ transformants has acquired S_6 specificity. The correlation of SCR_6 expression with gain of S_6 specificity not only proves the functional involvement of *SCR* in SI, but also demonstrates that this gene is sufficient for determining male SI specificity. With the identification of *SCR* as the male SI determinant, we can now define the *S* locus as a tightly linked genetic unit encompassing the array of *SLG/SRK* and *SCR* genes.

SCR as a Potential Ligand for the S-Locus Receptor Kinase

To analyze the structure and polymorphism of the *SCR* gene products, we compared the deduced amino acid sequences of the three

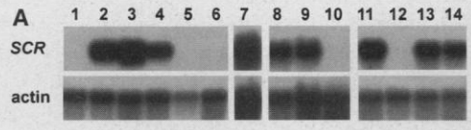

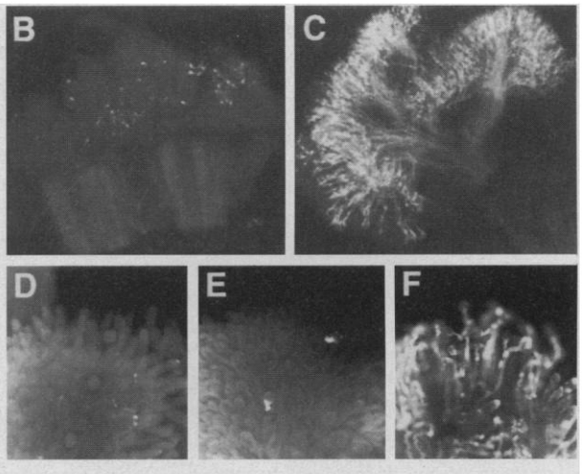

Fig. 3. Expression and functional analysis of *SCR*. (**A**) Gel blots of polyadenylated RNA were sequentially hybridized with an *SCR* probe (SCR_8 for lanes 1 to 7, SCR_{13} for lanes 8 to 10, SCR_6 for lanes 11 to 14) and a *Brassica* actin probe. Lanes 1 to 7 contain RNA isolated from *B. campestris* S_8S_8 plants: stigmas (lane 1), anthers of 2.5- to 3.9-mm buds containing uni- and binucleate microspores (lane 2), anthers of 4.0- to 5.0-mm buds containing bi- and trinuclear microspores (lane 3), anthers of 5.1- to 6.0-mm buds containing trinuclear microspores (lane 4), anthers of open flowers containing mature pollen grains (lane 5), leaves (lane 6), and microspores collected from 4.0- to 6.0-mm buds (lane 7). Lanes 8 to 10 contain anther RNA isolated from a self-incompatible *B. oleracea* $S_{13}S_{13}$ homozygote (lane 8), a self-incompatible $S_{13}S_{f1}$ heterozygote (lane 9), and the self-compatible mutant *m1600* (lane 10). Lanes 11 to 14 contain anther RNA from four representative S_2S_2 plants transformed with SCR_6, three of which express SCR_6 transcripts (lanes 11, 13, and 14) and one of which lacks SCR_6 transcripts (lane 12). (**B** to **F**) Pollination response of pollen from SCR_6 transformants on S_6S_6 stigmas. (B) Pollen from a transformant expressing SCR_6 [same plant as in (A), lane 11]. (C) Pollen from a transformant without detectable levels of SCR_6 transcript [same plant as in (A), lane 12]. Representative details of pollinated S_6S_6 stigmas display the incompatible reaction exhibited by pollen from S_6S_6 plants (D) and S_2S_2/SCR_6^+ plants (E), and the compatible reaction exhibited by pollen from S_2S_2/SCR_6^- plants (F). Absent or aborted short pollen tubes are indicative of an incompatible reaction and are clearly distinguished from the dense array of pollen tubes penetrating the stigma in a compatible reaction.

Table 1. Pollen phenotype of S_2S_2/SCR_6^+ and S_2S_2/SCR_6^- plants assayed on stigmas of S_6 and S_{22} homozygotes. The data represent the number of pollen tubes observed on S_6S_6 stigmas in at least three experiments performed on different dates, with each experiment consisting of two to three pollinated stigmas. Control pollinations with $S_{22}S_{22}$ stigmas were performed on two different dates.

♀ \ ♂	S_2S_2/SCR_6^+												S_2S_2/SCR_6^-		S_6S_6	S_2S_2	$S_{22}S_{22}$
	T1	T2	T3	T4	T5	T6	T7	T8	T9	T10	T11	T12	T13	T14			
S_6S_6	<6	<5	0	<16	0	<4	0	0	0	<6	<11	<6	>300	>300	0	>300	>300
$S_{22}S_{22}$	>300	>300	>300	>300	>300	>300	>300	>300	>300	>300	>300	>300	>300	>300	>300	>300	<3

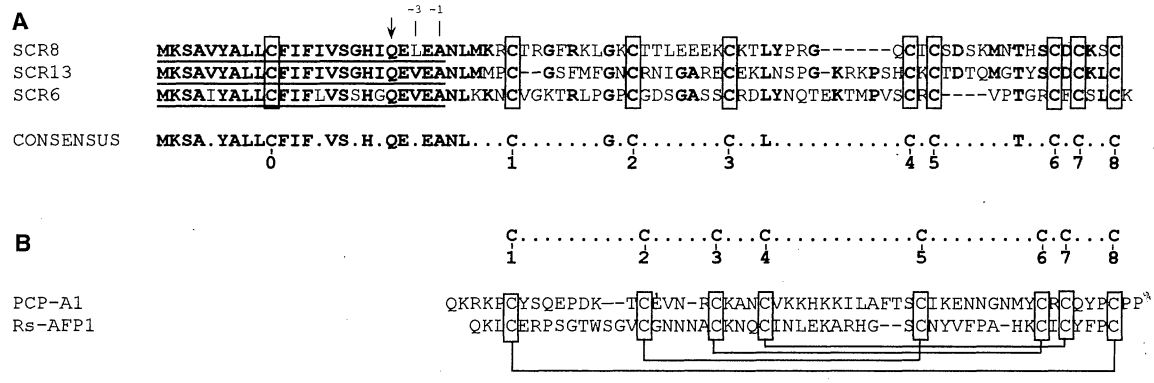

Fig. 4. (**A**) Amino acid sequence alignment of the predicted SCR_8, SCR_{13}, and SCR_6 proteins (GenBank accession numbers AF195627, AF195626, and AF195625, respectively). Gaps, represented by hyphens, were introduced to optimize the alignment. The arrow marks the conserved site of the intron, which has a length of 4.1 kb in SCR_8, but only 0.75 kb in SCR_{13} and 0.88 kb in SCR_6. The putative signal peptides are underlined. The two positions complying with the "(-3,-1)-rule" for signal peptides (*17*) are indicated. Bold letters mark amino acids that are identical in at least two sequences. A consensus sequence is shown with numbered cysteine residues. (**B**) Cysteine pattern in mature proteins of the PCP family, represented by PCP-A1 (*19*), and the plant defensins, represented by Rs-AFP1 (*21*). Lines indicate the disulfide bridges determined for Rs-AFP by x-ray crystallography. Abbreviations for the amino acid residues are as follows: A, Ala; C, Cys; D, Asp; E, Glu; F, Phe; G, Gly; H, His; I, Ile; K, Lys; L, Leu; M, Met; N, Asn; P, Pro; Q, Gln; R, Arg; S, Ser; T, Thr; V, Val; W, Trp; and Y, Tyr.

cloned *SCR* sequences (Fig. 4A). The *SCR* alleles encode polypeptides of 74 to 77 amino acids, which are hydrophilic except for an NH_2-terminal hydrophobic stretch of 19 amino acids (*16*). Based on the compliance of amino acid residues 24 and 26 in the SCR sequences with the "(-3,-1)-rule" for cleavage of signal peptides (*17*), we predict that the mature SCR proteins are small (8.4 to 8.6 kD), basic (isoelectric point 8.1 to 8.4), secreted proteins. Sequence comparison of the three SCR preproteins reveals that although conservation is high in the NH_2-terminal region extending two amino acids beyond the putative signal peptide cleavage site, conservation in the remaining sequence is limited to 11 amino acids, 8 of which are cysteines. Indeed, overall sequence identities are only 42, 30, and 37% for the pairwise comparisons SCR_8/SCR_{13}, SCR_8/SCR_6, and SCR_6/SCR_{13}, respectively. This extensive divergence of the SCR proteins is consistent with their role as male SI specificity determinants.

Database searches did not identify any significant homologies. However, small cysteine-rich proteins, the pollen coat proteins (PCPs), have been discussed previously as candidates for the male SI determinant (*18–20*). PCPs are basic 6 to 8-kD proteins with a cysteine pattern suggesting a cysteine-stabilized tertiary structure related to that of plant defensins (*21*). PCPs constitute the major component in a pollen coat fraction that was reported to modify pollen SI phenotype (*18*), but they lack both *S*-locus linkage and *S* haplotype–associated polymorphism. Therefore, the PCPs analyzed to date are unlikely to function in SI specificity. The predicted SCR proteins, even though resembling PCPs in charge and molecular size, have a distinct cysteine pattern that is most apparent when the spacing of cysteine residues Cys^3, Cys^4, and Cys^5 in SCR and the PCPs/defensins is compared (Fig. 4, A and B). Thus, SCRs represent a new class of small, secreted, cysteine-rich proteins, distinguishable from members of the PCP/defensin family. Nevertheless, we speculate that the even-numbered cysteine residues in mature SCR proteins are engaged in disulfide bridges, as has been shown for the cysteine residues of defensins and inferred for the ones of PCPs (*19*, *21*). Although a cysteine-stabilized three-dimensional structure may be common to SCR proteins, we expect the amino acid stretches between the cysteine residues, varying in length and composition between *SCR* alleles (Fig. 4A), to form loops at the surface of the folded protein. By imparting extensive structural diversity on the small SCR polypeptide molecules, such loops could mediate specificity in the SI recognition reaction.

Having established that the *SCR* gene determines pollen SI specificity, we suggest that the *SCR* gene product represents the pollen-borne ligand postulated to activate the stigmatic SRK receptor. The small hydrophilic polypeptide predicted by the *SCR* sequence is expected to localize to the pollen coat after its secretion from developing microspores [similar to the secretion of other gametophytically expressed components of the pollen coat (*19*)] and also possibly from cells of the tapetum. In either case, SCR molecules would mix readily within the anther locule and consequently, the pollen coat of all pollen grains in an *S*-locus heterozygote would incorporate SCR proteins encoded by each of the two parental *S* haplotypes, as predicted by sporophytic control of SI in *Brassica* (*22*). SCR would translocate into the cell walls of the stigma epidermal cell through the pollen coat–stigma contact zone. In the case of self-pollination, SCR would bind to a structurally complementary SRK receptor, resulting in activation of the receptor and initiation of a signal transduction cascade that ultimately leads to pollen inhibition.

References and Notes

1. J. B. Nasrallah, *Proc. Natl. Acad. Sci. U.S.A.* **94**, 9516 (1997); ———, J. C. Stein, M. K. Kandasamy, M. E. Nasrallah, *Science* **266**, 1505 (1994).
2. D. C. Boyes, M. E. Nasrallah, J. Vrebalov, J. B. Nasrallah, *Plant Cell* **9**, 237 (1997).
3. M. Kusaba, T. Nishio, Y. Satta, K. Hinata, D. Ockendon, *Proc. Natl. Acad. Sci. U.S.A.* **94**, 7673 (1997).
4. K. G. Dwyer, M. A. Balent, J. B. Nasrallah, M. E. Nasrallah, *Plant Mol. Biol.* **16**, 481 (1991).
5. J. C. Stein, R. Dixit, M. E. Nasrallah, J. B. Nasrallah, *Plant Cell* **8**, 429 (1996); R. Dixit, M. E. Nasrallah, J. B. Nasrallah, unpublished data.
6. K. Yu, U. Schafer, T. L. Glavin, D. R. Goring, S. J. Rothstein, *Plant Cell* **8**, 2369 (1996).

7. A. L. Casselman and J. B. Nasrallah, unpublished data.
8. J. A. Conner, P. Conner, M. E. Nasrallah, J. B. Nasrallah, *Plant Cell* **10**, 801 (1998).
9. cDNA libraries were constructed with the λUNIZAP phagemid system (Stratagene). Hybridization conditions for RNA and DNA gel blots were as described [D. C. Boyes, C.-H. Chen, T. Tantikanjana, J. J. Esch, J. B. Nasrallah, *Genetics* **127**, 221 (1991)] except that washes (each 20 min at 65°C) were extended by using successively 2× SET, 0.5% SDS and 1× SET, 0.1% SDS and 0.2× SET, and 0.1% SDS, unless indicated otherwise.
10. The S_2S_6 F_2 population was derived from a cross between *B. oleracea* S_6S_6 and S_2S_2 homozygotes. The genotypes and SI phenotypes of 153 individual plants had been determined previously. Gel blot analysis of Hind III–digested genomic DNA revealed coinciding hybridization patterns for SLG_6- and SCR_6-specific probes. All 116 plants hybridizing to SLG_6 also hybridized to SCR_6, whereas all 37 plants devoid of SLG_6 also lacked SCR_6. Similarly, 80 plants of an F_2 population segregating for S_6 and S_{13} were genotyped by hybridization of Hind III–digested genomic DNA with SLG_6- and SLG_{13}-specific probes. Hybridization with an SCR_{13}-specific probe revealed that 34 SLG_{13}-containing plants contained SCR_{13}, in contrast to 46 plants lacking both SLG_{13} and SCR_{13}.
11. The *B. campestris* S_9 haplotype also appears to contain an *SCR*-related sequence [G. Suzuki *et al.*, *Genetics* **153**, 391 (1999)].
12. Polyadenylated RNA was analyzed as in (*2*, *9*). Microspores were staged by DAPI (4′,6′-diamidino-2-phenylindole) staining [S. Detchepare, P. Heizmann, C. Dumas, *J. Plant Physiol.* **135**, 129 (1989)] and purified as described [D. C. Boyes and J. B. Nasrallah, *Plant Cell* **7**, 1283 (1995)].
13. J. B. Nasrallah *et al.*, *Ann. Bot.*, in press.
14. As host for the transformation of the SCR_6 cDNA, we chose a *B. oleracea* S_2S_2 homozygote. Besides ease of transformation and regeneration, this strain is expected to have an endogenous *SCR* allele with only low sequence similarity to the transgene, which reduces the risk of homology-dependent gene silencing (Fig. 2A). The transformation construct contained the SCR_6 cDNA preceded by the SCR_8 1.3-kb upstream region and followed by the nos terminator. After introducing appropriate restriction sites by polymerase chain reaction followed by DNA sequence analysis, both *SCR* fragments were assembled as a transcriptional fusion in pCR2.1 (Invitrogen) and subcloned as a 1.7-kb Hind III–Sac I fragment into pCAMBIA1300 upstream of an Eco RI–Sac I nos promoter. After mobilization into *Agrobacterium tumefaciens* strain GV3101, the construct was used for transformation of flower stem disks of the *B. oleracea* S_2S_2 strain, as described [K. Toriyama, J. C. Stein, M. E. Nasrallah, J. B. Nasrallah, *Theor. Appl. Genet.* **81**, 769 (1991)], applying hygromycin selection. The independent origin of the transformants was verified by DNA gel blot analysis.
15. Pollen was manually transferred onto stigmas of open flowers. After 7 to 9 hours, pollen tube growth was observed by ultraviolet fluorescence microscopy [Y. O. Kho and J. Baer, *Euphytica* **17**, 298 (1968)].
16. Open reading frames encoded by the three cDNAs SCR_8, SCR_{13}, and SCR_6 were identified on the basis of sequence similarity of the cysteine-rich reading frame, as well as the presence of stop codons upstream of the ATG initiation codon.
17. G. von Heijne, *Nucleic Acids Res.* **14**, 4683 (1986).
18. A. G. Stephenson *et al.*, *Plant J.* **12**, 1351 (1997).
19. J. Doughty *et al.*, *Plant Cell* **10**, 1333 (1998).
20. B. S. Stanchev, J. Doughty, C. P. Scutt, H. G. Dickinson, R. R. D. Croy, *Plant J.* **10**, 303 (1996).
21. W. F. Broekaert *et al.*, *Crit. Rev. Plant Sci.* **16**, 297 (1997); W. F. Broekaert, F. R. G. Terras, B. P. A. Cammue, R. W. Osborn, *Plant Physiol.* **108**, 1353 (1995); F. R. G. Terras *et al.*, *J. Biol. Chem.* **267**, 15301 (1992).
22. SI in *Brassica* is under sporophytic control, whereby pollen phenotype in *S*-locus heterozygotes is determined by the two *S* alleles carried by the diploid parent plant and not by the single *S* allele carried by the haploid pollen grain.
23. Supported by NIH grant GM57527, NSF grant IBN-9631921, and U.S. Department of Agriculture grant 98-358301-6072.

13 September 1999; accepted 26 October 1999

Molecular Architecture of the Rotary Motor in ATP Synthase

Daniela Stock,[1] Andrew G. W. Leslie,[2] John E. Walker[1]*

Adenosine triphosphate (ATP) synthase contains a rotary motor involved in biological energy conversion. Its membrane-embedded F_o sector has a rotation generator fueled by the proton-motive force, which provides the energy required for the synthesis of ATP by the F_1 domain. An electron density map obtained from crystals of a subcomplex of yeast mitochondrial ATP synthase shows a ring of 10 c subunits. Each c subunit forms an α-helical hairpin. The interhelical loops of six to seven of the c subunits are in close contact with the γ and δ subunits of the central stalk. The extensive contact between the c ring and the stalk suggests that they may rotate as an ensemble during catalysis.

ATP is the universal biological energy currency. ATP synthase produces ATP from adenosine diphosphate (ADP) and inorganic phosphate with the use of energy from a transmembrane proton-motive force generated by respiration or photosynthesis [for reviews, see (*1*–*3*)]. The enzyme consists of an extramembranous F_1 catalytic domain linked by means of a central stalk to an intrinsic membrane domain called F_0. The globular F_1 domain is an assembly of five different subunits with the stoichiometry $\alpha_3\beta_3\gamma_1\delta_1\varepsilon_1$. In the atomic structure of bovine F_1, the α and β subunits are arranged alternately around a coiled coil of two antiparallel α helices in the γ subunit. The catalytic sites are in the β subunits at the α/β subunit interface (*4*). The remainder of the γ subunit protrudes from the $\alpha_3\beta_3$ assembly and can be cross linked to the polar loop region of the c subunits in F_0 (*5*, *6*). In mitochondria, the δ and ε subunits are associated with the γ subunit in the central stalk assembly (*7*–*10*), as are the bacterial and chloroplast ε subunits, the counterparts of mitochondrial δ. ATP-dependent rotation of γ and ε within an immobilized $\alpha_3\beta_3$ complex from the thermophilic bacterium *Bacillus* PS3 has been observed directly (*11*, *12*). The rotation of the γ subunit in ATP synthase is thought to be generated by the passage of protons through F_0. Because there is only one intrinsically asymmetric γ subunit, it interacts differently with each of the three catalytic β subunits in F_1, endowing them with different nucleotide affinities (*4*). Rotation of the central stalk is accompanied by conformational changes in the β subunits, which cycle sequentially through structural states corresponding to low, medium, and high nucleotide affinities. These three states are probably associated with release of product (ATP), binding of substrates (ADP and inorganic phosphate), and ATP formation, respectively. The cycle is known as the "binding change mechanism" of ATP synthesis (*13*). In eubacteria, the procedure is reversible, and hydrolysis of ATP in F_1 generates rotation of γ, resulting in the pumping of protons back across the membrane through F_0 (*2*).

In contrast to the detailed structural model established for most of the bovine F_1 domain (*4*, *14*–*16*) and additional structural information in other species (*17*, *18*), little is known about the structural details of F_0. All species contain three common subunits known as a, b, and c. In *Escherichia coli*, the experimentally determined ratio of these subunits is $a_1b_2c_{9\text{-}11}$ (*19*, *20*). Cross-linking and genetic experiments (*21*, *22*), as well as evolutionary arguments (*23*), have been interpreted as showing the presence of 12 c subunits per F_0. From biochemical studies and mutational analysis in bacteria (*2*, *24*) and fungi (*25*), it is known that both a and c subunits contain functional groups that are essential for proton translocation through the membrane. A nuclear magnetic resonance (NMR) structure of a monomer of the *E. coli* c subunit in a chloroform:methanol:water mixture shows that the protein is folded into two α helices (presumed to be transmembrane in the intact enzyme), linked by a loop (presumed to be extramembranous) (*26*). The COOH-terminal α helix contains a conserved side chain carboxylate (Asp^{61} in *E. coli* and Glu^{59} in *Saccharomyces cerevisiae*) essential for proton translocation (*2*). Models have been proposed in which the a and b subunits are on the

[1]Medical Research Council Dunn Human Nutrition Unit, Hills Road, Cambridge CB2 2XY, UK. [2]Medical Research Council Laboratory of Molecular Biology, Hills Road, Cambridge CB2 2QH, UK.

*To whom correspondence should be addressed. E-mail: walker@mrc-dunn.cam.ac.uk

References and Notes

[1] **Evolution of the Brassica Self-Incompatibility Locus: A Look into S-Locus Gene Polymorphisms**

June B. Nasrallah

Proceedings of the National Academy of Sciences of the United States of America, Vol. 94, No. 18. (Sep. 2, 1997), pp. 9516-9519.

Stable URL:

http://links.jstor.org/sici?sici=0027-8424%2819970902%2994%3A18%3C9516%3AEOTBSL%3E2.0.CO%3B2-K

[1] **Signaling the Arrest of Pollen Tube Development in Self-Incompatible Plants**

J. B. Nasrallah; J. C. Stein; M. K. Kandasamy; M. E. Nasrallah

Science, New Series, Vol. 266, No. 5190. (Dec. 2, 1994), pp. 1505-1508.

Stable URL:

http://links.jstor.org/sici?sici=0036-8075%2819941202%293%3A266%3A5190%3C1505%3ASTAOPT%3E2.0.CO%3B2-D

[3] **Striking Sequence Similarity in Inter- and Intra-Specific Comparisons of Class I SLG Alleles from Brassica oleracea and Brassica campestris: Implications for the Evolution and Recognition Mechanism**

Makoto Kusaba; Takeshi Nishio; Yoko Satta; Kokichi Hinata; David Ockendon

Proceedings of the National Academy of Sciences of the United States of America, Vol. 94, No. 14. (Jul. 8, 1997), pp. 7673-7678.

Stable URL:

http://links.jstor.org/sici?sici=0027-8424%2819970708%2994%3A14%3C7673%3ASSSIIA%3E2.0.CO%3B2-7